Experimental Characterisation of a Positive Displacement Pump-Turbine for Low-Head Pumped Hydro Storage

Journal of Physics: Conference Series **3185** (2026) 012016 doi:10.1088/1742-6596/3185/1/012016

Experimental Characterisation of a Positive Displacement Pump-Turbine for Low-Head Pumped Hydro Storage

A. Jarquin-Laguna[1], J.P. Hoffstaedt[1], R. Ansorena Ruiz[2], D. Schürenkamp[2] and N. Goseberg[2]

[1]Department of Maritime and Transport Technology, Faculty of Mechanical Engineering, Delft University of Technology, the Netherlands.
[2]Leichtweiß-Institute for Hydraulic Engineering and Water Resources, Technische Universitaet Braunschweig, Germany.

E-mail: a.jarquinlaguna@tudelft.nl

Abstract. Pumped hydropower provides the largest form of grid-scale energy storage. It plays a key role in the integration of variable renewables like wind and solar energy, and contributes to enhancing grid reliability. A great interest exists towards the exploitation of low head differences, particularly in shallow seas and environments with flat topography. This work presents an experimental analysis of the efficiency and operational performance of a 7 kW positive displacement reversible pump-turbine (PD-RPT) designed for low-head hydro applications under steady-state conditions. The PD-RPT features two rotors with three lobes and cycloidal surfaces. The characterisation tests were carried out in the hydraulic laboratory of TU Braunschweig for turbine and pump modes under variable speed conditions. The results highlight experimental peak efficiencies of 74.7% in turbine mode and 74.0% in pump mode for the operational range tested. In addition to challenges in efficiency and operational flexibility, the PD-RPT experiments also showed the need for effective debris management strategies to avoid performance degradation.

1 Introduction

Hydropower remains the largest renewable source of electricity worldwide, serving as a cornerstone of the global transition to sustainable energy. Beyond generating power, hydropower has long utilized pumped hydro storage (PHS) to store excess energy and release it during peak demand, enhancing grid reliability. With the rise of intermittent renewable sources such as wind and solar, PHS has played an even greater role in stabilizing the grid [1]. However, as high-elevation reservoirs become increasingly used, attention is turning to low-head applications, particularly in shallow seas and environments with flat topography and heights up to 20 m [2]. This shift presents distinct challenges, as traditional fluid machinery designed for high-head applications proves unsuitable. Very low-head turbines have been studied and developed, but these devices generally lack the pumping capability [3, 4].To address this gap, innovative reversible pump-turbine technologies are emerging, offering new opportunities for sustainable energy storage in low-head and coastal environments [5].

Low-head PHS systems require pumps and turbines that maintain high efficiency across variable low-head and discharge conditions. At grid scale, traditional machines such as bulb and Kaplan turbines

have been used in tidal and low-head applications, but face limitations: bulb turbines show poor pump-mode efficiency [6], and Kaplan turbines, while adaptable, struggle with large discharges and long-term fatigue [7, 8]. Axial-flow counter-rotating pump turbines have emerged as promising alternatives, offering compactness, broader efficiency ranges, and independent runner control [9–11]. Additionally, unconventional machines like Archimedes screws [12–14], and positive displacement pumps are being explored for specialised low-head applications due to their operational and environmental benefits [15].

Positive displacement (PD) machines offer stable performance across varying heads, and the ability to handle viscous or particle-laden fluids, making them well suited for low-head PHS. Although they require significantly larger dimensions to meet flow demands in low-head applications, their self-priming nature and operational robustness remain advantageous. In environmentally sensitive seawater PHS systems, rotary lobe pumps are especially promising due to their gentle handling of aquatic life. Previous studies have demonstrated their effectiveness as turbine in small-scale hydro applications, supporting their potential in scalable, sustainable energy storage solutions [16, 17].

This work presents an experimental approach to quantify the efficiency of a positive displacement reversible pump-turbine (PD-RPT) designed for low-head hydro applications under steady-state conditions. The PD-RPT machine was tested in the context of the ALPHEUS European project on low head pumped hydro energy storage [18]. Experiments were carried at the hydraulic laboratory of the Technische Universität Braunschweig (TUB) in Germany, for both pump and turbine operation as shown in Figure 1.

Figure 1: Side view of the PD-RPT unit during a wet test run at the TUB hydraulic lab.

2 Experimental facility

2.1 Description of the model

The studied PD-RPT features two rotors with three lobes and cycloidal surfaces, each having a diameter of $D = 0.349$ m, a rotor length of $L = 0.30$ m, a rotor-rotor distance of $d_{rr} = 0.263$ m, with tip and side gaps equal to g_{rr} =0.15 mm. In the absence of leakages, the geometry results in a volumetric displacement of $V_d = 22.14$ litres per revolution. A circular pipe is used to transition in shape to a rectangular profile to match the height of the rotors. Due to the positive displacement design and intersection of the lobes, their rotational motion is linked via gears attached to both lobes. Consequently, there is only one driveshaft, and the device was designed such that it could be tested using a 37 kW 6-pole electrical machine that can operate both as motor and generator. The housing and rotors were machined in aluminium from four separate rectangular blocks. Figure 2 illustrates the 3D design and the device constructed and assembled.

2.2 Hydraulic lab setup

The experimental setup was constructed at the Leichtweiß-Institute for Hydraulic Engineering and Water Resources of the TUB in Germany. The setup consists of two open surface tanks, which represent the upper and lower reservoir found in PHS applications. The lower tank features an adjustable spillway and

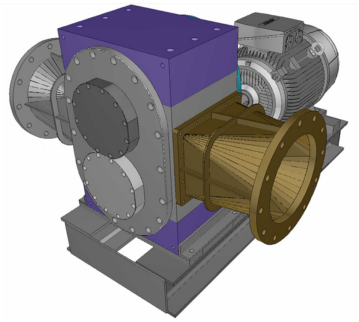

(a) 3D CAD of the PD-RPT.

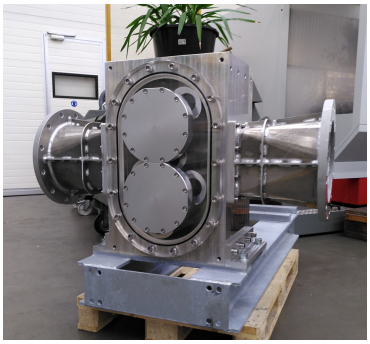

(b) Photo of the constructed PD-RPT.

(c) Hollow rotor lobes with cycloidal surfaces.

Figure 2: 3D illustration and final fabrication of the PD-RPT device.

both tanks are connected via two pipes; the first incorporating the PD-RPT device as shown in Figure 3. The water level of the elevated tank is 9.7 m above the centre line of the device, while the lower tank level is between 1.25 and 2.25 m above the centre line, resulting in an available gross head between 7.45 and 8.45 m. The pipes have a diameter of 0.5 m, tapering to 0.276 m via two contraction/expansion sections which are designed at a 4-degree angle to prevent and reduce flow separation. This configuration allows for a maximum flow rate of approximately 400 l/s. A butterfly valve is positioned between the elevated tank and the PD-RPT, with the aim to enable manual control of the discharge flow, nevertheless, it can also alter the net head over the PD-RPT. The setup is designed to facilitate testing in both turbine and pump modes. In turbine mode, the flow goes from the elevated tank to the lower tank through the PD-RPT in pipe 1, while pipe 2 remains closed. In pump mode, pipe 2 is opened, which allows a flow from the elevated tank to maintain a stable water level in the lower tank. In both modes, water is pumped from an underground reservoir to the elevated tank via the laboratory supply system. The elevated tank is equipped with a sharp-edged weir to maintain the water level in order to ensure a constant head throughout the experiments.

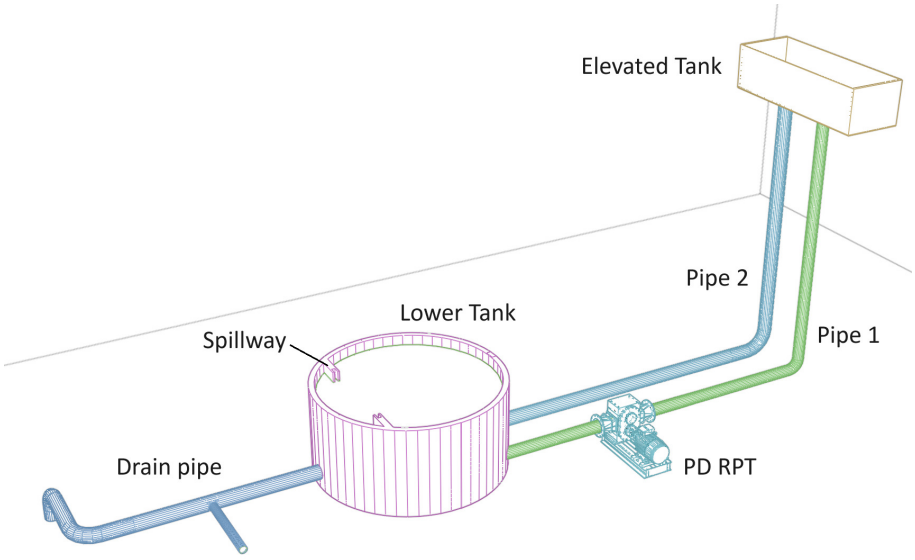

Figure 3: Schematic overview of the TUB laboratory setup for the PD-RPT experiments.

2.3 Instrumentation and data acquisition

The setup is equipped with a range of sensors to record data on the flow characteristics (pressure and flow rates) and machine operation (torque and rotational speed). The 12 pressure probes, denoted with p1 to p12, are located in six different axial locations, as depicted in Figure 4. The pressure measurements are averaged for every pair of probes at each location. The difference between probe pairs p7 & p8 and p5 & p6 is used to obtain the PD-RPT net head. Additionally, probe pairs are located before (p3 & p4 and p9 & p10) as well as after (p1 & p2 and p11 & p12) the contraction and expansion tubes. An electromagnetic flow meter is located between the butterfly valve and the PD-RPT to prevent disturbance of the flow. The torque is measured using a torque transducer in the driving shaft of the electrical machine.

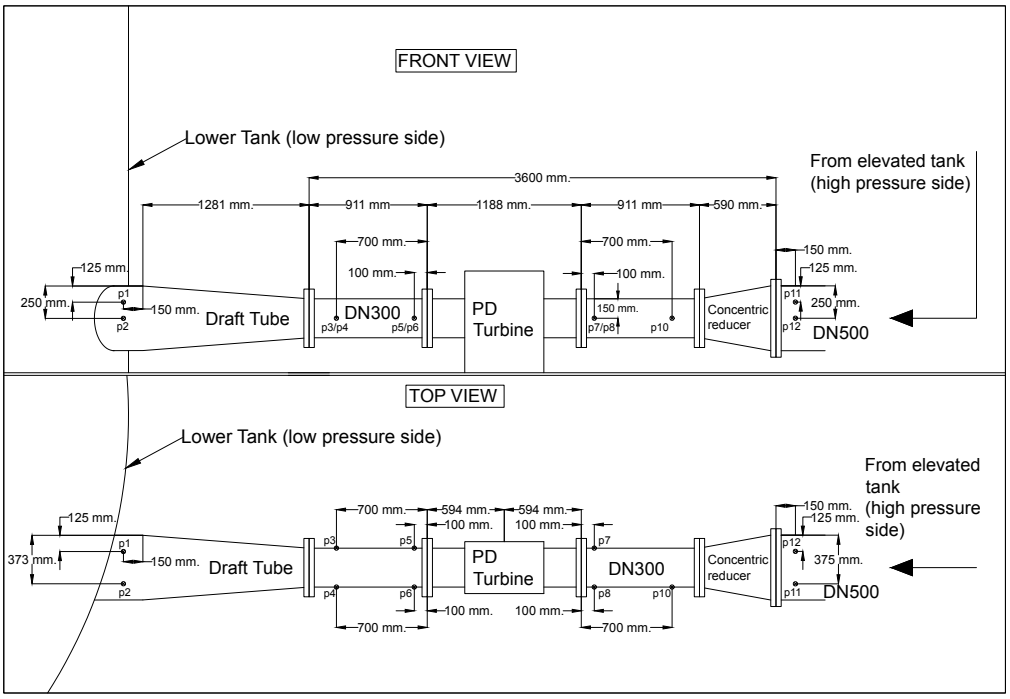

Figure 4: Schematic of the positioning of the pressure probes for the PD-RPT.

The analog signals from the flow meter, torque transducer, and pressure sensors are connected through a Data Acquisition System (DAS) to a PC, facilitated by the software GI.Bench v1.13. Moreover, a MicroLabBox controller inputs data from the encoders into a separate PC which operates the electrical machine. In this way, using voltage and frequency, the control unit of the electrical drive obtains the rotational speed of the electric machine, which is also sent to the PC system. To synchronize data acquisition with MicroLabBox and the DAS, an electric signal is sent simultaneously to both systems to trigger data recording. Data recording, visualisation, and output is performed using the software ControlDesk v7.1. A sampling rate of 10 Hz, was used for steady-state measurements. Further details on the instrumentation equipment is found in Appendix A.

3 Performance characterisation

3.1 Power measurements

Steady-state tests were conducted for the PD-RPT with the goal of obtaining its efficiency in both turbine and pump mode. In turbine mode, the hydraulic power, P_{hyd}, available to the PD-RPT is given by the product of the volumetric flow rate Q and the net pressure across the device, as expressed in Equation (1):

$$P_{hyd} = \rho\, g\, Q\, H \tag{1}$$

where, ρ (kg/m^3) is the density of water, g (m/s^2) the gravitational acceleration, and H (m) the net head, representing the difference in water levels upstream and downstream of the PD-RPT device. In pump mode, this expression is used to obtain the hydraulic power generated by the device. The net head is calculated from the difference between the pressure at the pipe's centreline at the p7 & p8 position

and that of p5 & p6. Notice that p5 and p7 give the pressure at the pipe's centreline but p6 and p8 at 13 cm below it. Therefore, their readings were adjusted by this height in order to obtain the static pressure given by p6 and p8 at the centreline of the pipe. After this adjustment, both pressure values were averaged. In addition, periodic signals were time averaged over one rotation cycle of the device to account for fluctuations as a result of the lobe interactions. In particular, this was the case for the torque measurements. Thus, the average mechanical power, P_{mech}, was obtained using the following equation:

$$P_{mech} = \frac{1}{T}\int_{t}^{t+T} \tau(t)\,\omega(t)\,dt \tag{2}$$

where T denotes the time period of a single rotor cycle, $\tau(t)$ is the instantaneous total torque of the PD-RPT machine and $\omega(t)$ is the rotational speed of the PD-RPT drive shaft.

3.2 Hydraulic efficiencies

With the hydraulic and mechanical power, the average PD-RPT hydraulic efficiency is calculated for both turbine η_{turbine} and pump mode η_{pump}. The efficiency η can be further separated into a volumetric and a hydromechanical efficiency [19].

$$\eta_{\text{turbine}} = \frac{P_{mech}}{P_{hyd}} = \left(\frac{\tau}{\rho\, g\, H\, V_d}\right)\left(\frac{V_d\,\omega}{Q}\right) = \eta_{\text{hydromech}}\,\eta_{\text{vol}} \tag{3}$$

$$\eta_{\text{pump}} = \frac{P_{hyd}}{P_{mech}} = \left(\frac{\rho\, g\, H\, V_d}{\tau}\right)\left(\frac{Q}{V_d\,\omega}\right) = \eta_{\text{hydromech}}\,\eta_{\text{vol}} \tag{4}$$

The volumetric efficiency, η_{vol} accounts for internal flow leakages and losses. It is defined as the measured flow rate divided by the expected theoretical flow rate as a function of the rotational speed and the volumetric displacement V_d. The hydromechanical efficiency, $\eta_{\text{hydromech}}$ accounts for the fluid pressure losses of the machine as well as for internal mechanical friction from gears and seals.

3.3 Dimensionless parameters used for performance evaluation

The performance analysis of the PD-RPT device is evaluated from the efficiency as a function of non-dimensional groups: the flow coefficient, ϕ, the head coefficient, ψ (also known as energy coefficient) and the power coefficient $\hat{P}$ as defined in Equation (5) for a positive displacement machine.

$$\phi = \frac{Q}{\omega D^2 L}, \qquad \psi = \frac{gH}{(\omega D)^2}, \qquad \hat{P} = \frac{P_{mech}}{\rho\,\omega^3 D^4 L} \tag{5}$$

Where the geometric parameters D and L are respectively the rotor diameter and axial length. This approach allows to standardise data across different flow rates, heads, and rotational speeds, enabling effective comparison and generalisation [20]. The Reynolds number, $Re = \rho\, UD/\mu$, was also evaluated to assess the viscous effects.

Another non-dimensional parameter called specifc speed,ω_s, was obtained to characterise the operational range where the best efficiency points occur. Since ω_s depends only on the operating parameters and it is independent of the characteristic diameter of the machine, it is very useful to provide the requirement of high efficiency at the design conditions, as well as to compare with other types of hydraulic machines. When the maximum efficiency η_{max} occurs at a unique value of flow coefficient $\phi = \phi_1$ and corresponding unique values of $\psi = \psi_1$ and $\hat{P} = \hat{P}_1$, it is possible to combine these coefficients to eliminate the diameter from the expressions given by Equation 5. A distinction is made between turbine and pump operation. In pump mode, the specific speed ω_s is defined by the operating point giving maximum efficiency such that,

$$\omega_s = \frac{\phi_1^{1/2}}{\psi_1^{3/4}} = \frac{\omega Q^{1/2}}{(gH)^{3/4}} \tag{6}$$

In the case of a hydraulic turbine, the power specific speed ω_{sp} is often used and is given by

$$\omega_{sp} = \frac{\hat{P}_1^{1/2}}{\psi_1^{5/4}} = \frac{\omega\,(P_{mech}/\rho)^{1/2}}{(gH)^{5/4}} \tag{7}$$

For a hydraulic turbine, the relation between specific speeds is given by the efficiency such that $\omega_{sp}/\omega_s = \sqrt{\eta_{\text{turbine}}}$.

4 Steady-state results

In the experimental tests, four parameters are measured: head, flow rate, rotational speed, and torque. With these parameters, the performance of the device was characterised in both turbine and pump mode. In all tests, the relative head of the setup was relatively constant, with head values ranging between 7.6 and 8.1 m. Therefore, the rotational speed of the device was modified through the electrical machine to cover different operating conditions. During turbine mode, measured data was averaged in intervals of 40 s duration, while during pump mode, it was averaged in 25 s intervals for every steady-state set point.

4.1 Turbine mode

In turbine mode, the operating range was constrained by the maximum torque of the electrical machine, where rotational speeds between 50 rpm and 400 rpm were tested. With a fully open valve, discharges between around 30 l/s and 163 l/s were achieved, resulting in Reynolds numbers 1.1e5< Re <6e5. The consequent net head over the PD-RPT ranged from 7.59 m to 7.71 m accounting for hydraulic losses. The average, standard deviation and maximum torques are illustrated in Figure 5a, where the inherent pulsating nature of the PD-RPT machine is clearly shown from the difference between the torques. An increase in absolute and relative values between the maximum and average torques is observed as the rotational speed increases. Mechanical power and efficiency are shown in Figure 5b, a clear maxima are observed for both. The average mechanical power in turbine mode ranged from 1.4 kW to 5.7 kW with the best efficiency of 74.7%, achieved at 150 rpm with 3.9 kW of power production, while a maximum mean mechanical power of 5.7 kW was obtained at 300 rpm, with an efficiency of 60.9%.

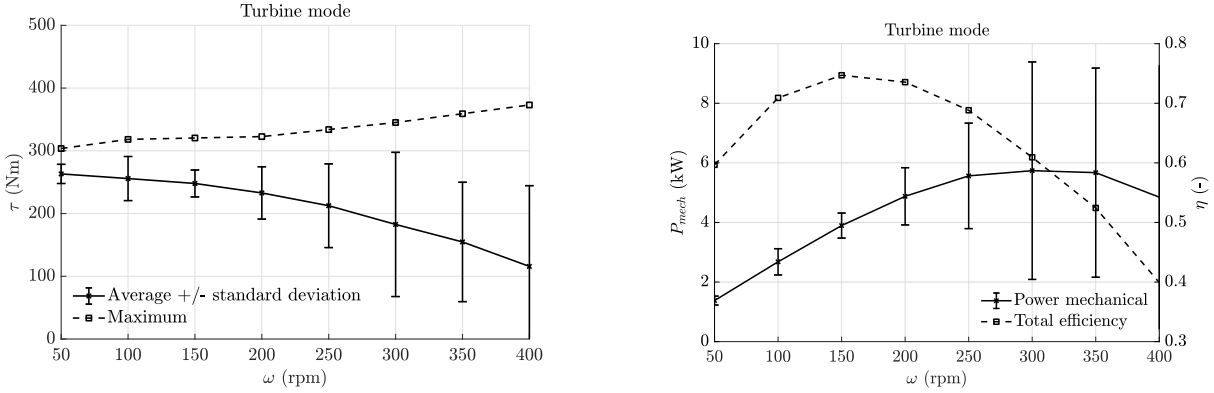

(a) Torque (b) Mechanical Power

Figure 5: Torque and mechanical power of the PD-RPT device in turbine mode.

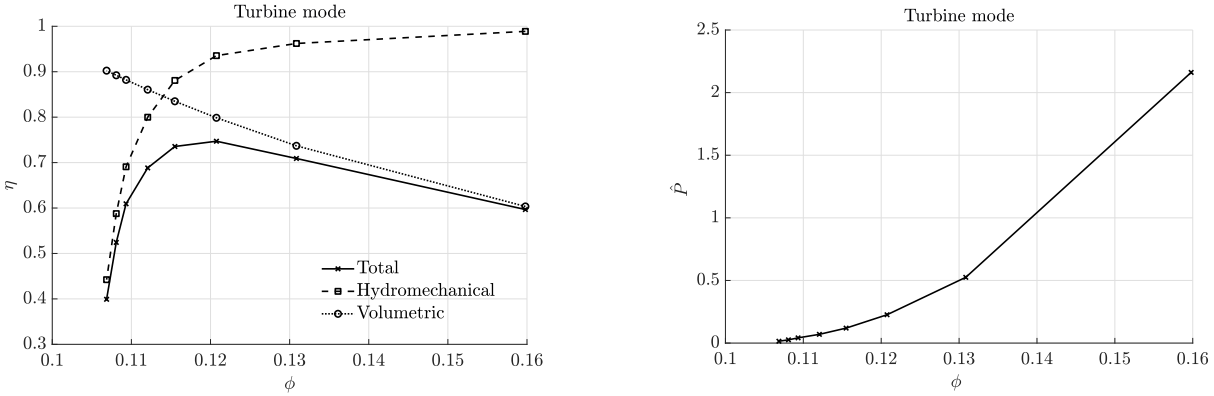

(a) ϕ vs η (b) ϕ vs $\hat{P}$

Figure 6: Efficiency and power coefficient of the PD-RPT device in turbine mode.

The performance characteristic curves of the turbine operation are illustrated in Figure 6 using dimensionless parameters. The average efficiency η and power coefficient $\hat{P}$, are shown as a function of the flow coefficient ϕ. It is important to note that the head or energy coefficient ψ can be obtained from the relation $\hat{P} = \eta\,\phi\,\psi$ for turbine mode. From Figure 6a, it is observed that at lower flow coefficients, leakage losses dominate compared to pressure and internal friction losses from seals and bearings. As the rotational speed increases and consequently the flow coefficient, the pressure and internal friction losses become more dominant and have a higher effect on the machine total efficiency.

4.2 Pump mode

Similarly, the steady-state results for the PD-RPT device in pump mode were obtained. Only a limited set of operational points were tested due to limitations from cavitation and associated structural vibrations occurring at rotational speeds above 200 rpm. Additionally, a minimum speed of 70 rpm was required to reach stable operation. The resulting flow rates ranged between 15 l/s to 67 l/s with corresponding Reynolds 5.7e4< Re <2.4e5, and net heads between 7.75 m to 7.78 m. Figure 7a shows that higher average torques and higher maxima were obtained compared to the turbine mode, although with lower fluctuations. The mechanical power required in pump mode was between 2.2 kW and 6.9 kW. The resulting hydraulic power and the efficiency of the machine are shown as a function of the rotational speed in Figure 7b. Despite the narrow operating range, the total efficiencies displayed were within 54% and 74% with resulting mean hydraulic power between 1.2 kW and 5.1 kW.The highest efficiency was shown at 200 rpm with a total efficiency of 74% requiring 6.9 kW of mechanical power on average.

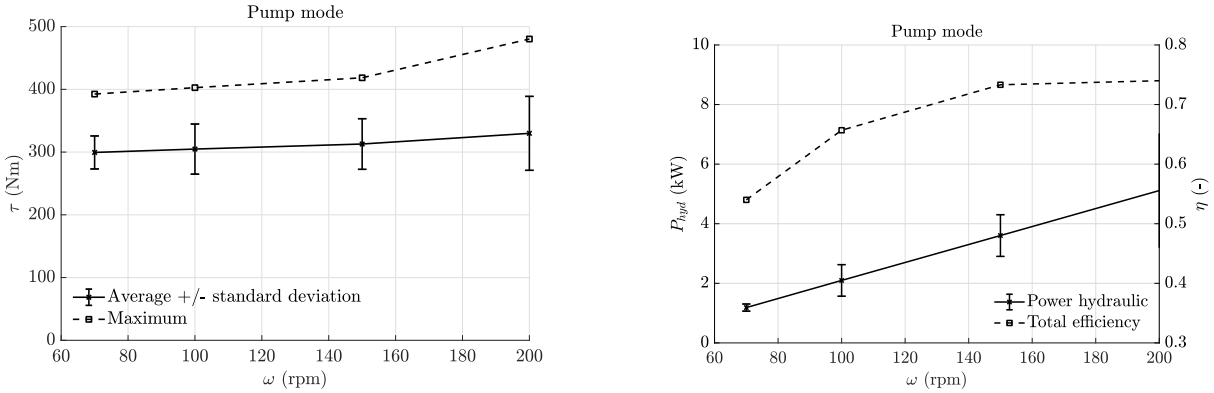

(a) Torque (b) Hydraulic Power

Figure 7: Torque and hydraulic power of the PD-RPT device in pump mode.

Regarding the performance characterisation, a lower range of flow coefficients was observed in pump mode due to the lower rotational speed compared to turbine operation. A counteracting trend is observed between volumetric and hydromechanical efficiencies as shown in Figure 8a. At lower speeds the pressure and friction losses are low compared to the leakage losses, while at higher speeds the opposite behaviour is observed. In pump mode, the head coefficient is of particular relevance and it is depicted in Figure 8b, where decreasing values between 1.4 and 11.6 are observed. In pump mode there is a different relation between the efficiency and the power coefficient $\hat{P}$, which can be obtained from the relation $\hat{P} = \frac{1}{\eta}\,\phi\,\psi$.

4.3 Damage to the PD-RPT during operation and cavitation

The PD-RPT was assembled with a tight clearance to minimise leakage and improve efficiency. However, the presence of debris particles in the hydraulic circuit caused damage and eventually led to the device seizing. Filtering to remove particles was not feasible due to increased hydraulic losses and shared water use. Incorporating sacrificial components or increasing the clearances could mitigate damage, though the latter would result in an undesirable reduction of volumetric efficiency. This debris issue is expected to be more significant in full-scale plants and requires further attention. Despite this, the planned testing was completed, and the steady-state performance was characterised in both turbine and pump modes.

The PD-RPT operational range in pump mode was largely restricted from high rotational speed, by the presence of cavitation due to a reduced static head at the low-pressure side of the device. This issue can be mitigated by optimizing inlet hydraulic conditions to maintain adequate pressure and prevent

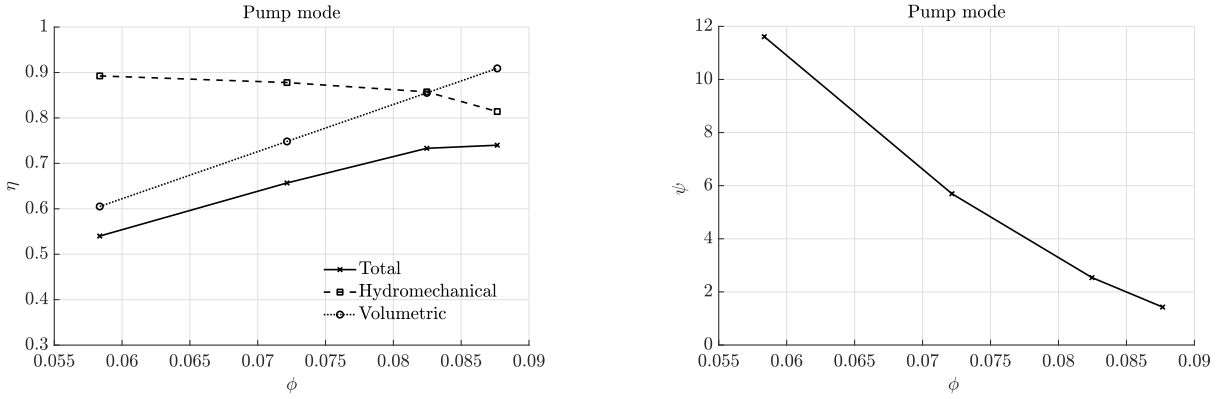

(a) ϕ vs η (b) ϕ vs ψ

Figure 8: Efficiency and head coefficient of the PD-RPT device in pump mode.

vapor formation. Additionally, implementing anti-cavitation control strategies and conducting transient CFD simulations can help better understand and minimize cavitation effects. Similar approaches have been developed for other reversible pump-turbine technologies [9] and can also be applied to the PD-RPT device.

4.4 Best efficiency points

A summary of the best efficiency points in turbine and pump mode is given in Table 1. Maximum averaged efficiencies of 75% and 74% were found in turbine and pump mode, respectively. These experimental findings show lower efficiency values compared to the numerical results reported in [15]. For the same PD-RPT geometry, two-dimensional CFD simulations predicted average efficiencies ranging from 80% to 92%. The discrepancy with experimental results is primarily due to the exclusion of internal friction losses from gears, seals, and bearings in the numerical model. Additionally, the simulations underestimate three-dimensional leakage effects. Enhancing CFD models with three-dimensional multiphase flow as well as fluid–structure interaction effects to predict cavitation and vibrations, would significantly improve numerical accuracy and reduce discrepancies with the experimental results presented in this study. Despite these limitations, the predicted machine behaviour and performance trends align well with the experimental observations.

Table 1: Best efficiency points for the tested operational range of the PD-RPT in steady-state conditions. All quantities are average values over one rotation cycle of the device.

Mode	**Efficiency** $\eta_{\max}$ [%]	**Speed** n_{BEP} [rpm]	**Flow rate** Q_{BEP} [l/s]	**Net head** H_{BEP}[m]	**(Power) specific speed** ω_{sp} or ω_s [-]
Turbine	74.7	150	69	7.71	0.15
Pump	74.0	200	67	7.78	0.23

Although the PD-RPT achieved experimental efficiencies above 70% in both pump and turbine mode, these values are well below those reported by other pump-turbine technologies. Counter-rotating pump turbines reported efficiencies of 88% in turbine mode and 86% in pump mode using the same experimental facility [10]. Archimedes screw turbines show efficiency values above 80% [13, 14]. The lower efficiency of the PD-RPT compared to other pump-turbine technologies implies higher energy losses during operation, which may limit its competitiveness for large-scale energy storage applications. However, its mechanical simplicity and suitability for low-head environments may still justify further development, particularly if design improvements can enhance overall performance.

5 Conclusions

This study has presented the experimental characterisation of a positive displacement reversible pump-turbine aimed at advancing low-head PHS technologies. Experiments provided insight into the steady-state performance and operational limitations of a 7 kW PD-RPT under variable speed conditions. At low specific speeds, the PD-RPT achieved peak efficiencies of 74.7% in turbine mode and 74% in pump mode, in Reynolds above 1e5. Hydromechanical losses were predominant at low rotational speeds, while leakage losses became significant at higher speeds despite the use of minimal clearances between the lobes and casing. However, the device exhibited a limited operational range in pump mode, constrained by cavitation and resulting vibrations at high speeds as well as torque limitations. A critical challenge encountered during testing was the presence of debris in the hydraulic circuit, which caused physical damage to the machine. This underscores the importance of incorporating effective debris mitigation strategies, either through filtration systems or more robust designs capable of tolerating particle-laden flows, especially for large scale deployments where water quality control is limited. Overall, the findings provide important guidance for future design and deployment of positive displacement RPTs in low-head PHS applications, highlighting the technical challenges in terms of performance and robustness that must be addressed for scalable implementation.

Appendix A
Instrumentation

The following instrumentation was employed in the experimental setup:

Table 2: Overview of sensors and transducers used in the experimental setup.

Measurement	**Type**	**Range**	**Accuracy**	**Model and manufacturer**
Flow rate	Electromagnetic	0 – 600 l/s	±0.312%	Krohne OPTIFLUX 2000
Pressure (p1–p6)	Piezoresistive	-0.5 – 0.35 bar	±0.1%	Druck Limited PDCR 1830
Pressure (p7,p9,p10,p12)	Piezoresistive	0 – 2.4 bar	±0.25%	BD Sensors DMP 321
Pressure (p8,p11)	Piezoresistive	-0.5 – 5 bar	±0.1%	Druck Limited PDCR 830
Torque	Strain gauge torque-transducer	-500 – 500 Nm	±0.5%	HBM T22
Rotational Speed	Motor-Generator Drive	-1500 –1500 rpm	±0.05%	Siemens Sinamics S120
Data Acquisition System	–	–	±0.04%	Gantner XL A108

Acknowledgement

This research is part of the ALPHEUS project, which has received funding from the European Union's Horizon 2020 research and innovation programme under grant agreement No. 883553. The authors would also like to thank DEMO from TU Delft for the technical support with the construction of the PD-RPT. A special thanks to the technicians and support staff from the hydraulic laboratory of TU Braunschweig.

References

[1] W. Yang, Z. Zhao, J. I. Pérez-Díaz, J. D. Hunt, E. Vagnoni, J. K. Nøland, E. Quaranta, R. Wang, X. Li, and Y. Cheng, "Pumped storage hydropower operation for supporting clean energy systems," *Nature Reviews Clean Technology*, pp. 1–20, 2025.

[2] E. Prasasti, M. Aouad, M. Joseph, M. Zangeneh, and K. Terheiden, "Optimization of pumped hydro energy storage design and operation for offshore low-head application and grid stabilization," *Renewable and Sustainable Energy Reviews*, vol. 191, p. 114122, 2024.

[3] E. Quaranta, A. Bahreini, A. Riasi, and R. Revelli, "The very low head turbine for hydropower generation in existing hydraulic infrastructures: State of the art and future challenges," *Sustainable Energy Technologies and Assessments*, vol. 51, p. 101924, 2022.

[4] A. Bahreini, A. Riasi, E. Quaranta, and M. Araghi, "Comparative study on the performance, flexibility, and flow characteristics of very low head turbines: Numerical and experimental insights into original model and its optimized variant," *Energy*, p. 136703, 2025.

[5] J. P. Hoffstaedt, D. Truijen, J. Fahlbeck, L. H. A. Gans, M. Qudaih, A. J. Laguna, J. De Kooning, K. Stockman, H. Nilsson, P.-T. Storli *et al.*, "Low-head pumped hydro storage: A review of applicable technologies for design, grid integration, control and modelling," *Renewable and Sustainable Energy Reviews*, vol. 158, p. 112119, 2022.

[6] C. H. Lebarbier, "Power from tides—the rance tidal power station," *Naval Engineers Journal*, vol. 87, no. 2, pp. 57–71, 1975.

[7] F. Gerini, E. Vagnoni, M. Seydoux, R. Cherkaoui, and M. Paolone, "Experimental investigation of repurposed Kaplan turbines as variable-speed propellers for maximizing frequency containment reserve," *Electric Power Systems Research*, vol. 235, p. 110718, 2024.

[8] E. Quaranta, M. Bonjean, D. Cuvato, C. Nicolet, M. Dreyer, A. Gaspoz, S. Rey-Mermet, B. Boulicaut, L. Pratalata, M. Pinelli *et al.*, "Hydropower case study collection: Innovative low head and ecologically improved turbines, hydropower in existing infrastructures, hydropeaking reduction, digitalization and governing systems," *Sustainability*, vol. 12, no. 21, p. 8873, 2020.

[9] J. Fahlbeck, H. Nilsson, M. H. Arabnejad, and S. Salehi, "Performance characteristics of a contra-rotating pump-turbine in turbine and pump modes under cavitating flow conditions," *Renewable Energy*, vol. 237, p. 121605, 2024.

[10] R. A. Ruiz, D. Schürenkamp, D. P. Truijen, J. P. Hoffstaedt, A. J. Laguna, J. Fahlbeck, H. Nilsson, M. Joseph, M. Zangeneh, J. D. De Kooning *et al.*, "Performance evaluation of a variable-speed contra-rotating pump-turbine for low-head pumped hydro energy storage: An experimental study," *Energy Conversion and Management: X*, vol. 26, p. 101009, 2025.

[11] D. P. Truijen, J. P. Hoffstaedt, J. Fahlbeck, A. J. Laguna, H. Nilsson, K. Stockman, and J. D. De Kooning, "Impact of dual variable speed and inlet valve control on the efficiency and operating range of low-head contra-rotating pump-turbines," *Ieee Access*, 2024.

[12] S. Waters and G. A. Aggidis, "Over 2000 years in review: Revival of the archimedes screw from pump to turbine," *Renewable and Sustainable Energy Reviews*, vol. 51, pp. 497–505, 2015.

[13] J. Rohmer, D. Knittel, G. Sturtzer, D. Flieller, and J. Renaud, "Modeling and experimental results of an archimedes screw turbine," *Renewable energy*, vol. 94, pp. 136–146, 2016.

[14] P. Sołowiej and K. Łapiński, "Recent progress in research on the design and use of an archimedes screw turbine: A review," *Sustainability*, vol. 17, no. 1, p. 201, 2025.

[15] L. H. A. Gans, "Design study of a reversible lobe pump-turbine for low-head seawater pumped hydro storage applications," Ph.D. dissertation, Norwegian University of Science and Technology NTNU, 2024.

[16] J. Kurokawa, J. Matsui, and Y.-D. Choi, "Flow analysis in positive displacement micro-hydro turbine and development of low pulsation turbine," *International Journal of Fluid Machinery and Systems*, vol. 1, no. 1, pp. 76–85, 2008.

[17] A. Sonawat, S.-J. Kim, H.-M. Yang, Y.-S. Choi, K.-M. Kim, Y.-K. Lee, and J.-H. Kim, "Positive displacement turbine-a novel solution to the pressure differential control valve failure problem and energy utilization," *Energy*, vol. 190, p. 116400, 2020.

[18] ALPHEUS, "Augmenting grid stability through low head pumped hydro energy utilization and storage.alpheus h2020," last accessed 05 May 2025. [Online]. Available: https://alpheus-h2020.eu/

[19] H. Kauranne, "Effect of operating parameters on efficiency of swash-plate type axial piston pump," *Energies*, vol. 15, no. 11, p. 4030, 2022.

[20] M. Amelio, S. Barbarelli, and D. Schinello, "Review of methods used for selecting pumps as turbines (pats) and predicting their characteristic curves," *Energies*, vol. 13, no. 23, p. 6341, 2020.